Feshbach resonances, molecular bound states, and prospects of ultracold-molecule formation in mixtures of ultracold K and Cs

Hannah J. Patel,[1] Caroline L. Blackley,[1] Simon L. Cornish,[2] and Jeremy M. Hutson[1]
[1]*Joint Quantum Centre (JQC) Durham/Newcastle, Department of Chemistry, Durham University, Durham DH1 3LE, United Kingdom*
[2]*Joint Quantum Centre (JQC) Durham/Newcastle, Department of Physics, Durham University, Durham DH1 3LE, United Kingdom*
(Received 24 July 2014; published 25 September 2014)

We consider the possibilities for producing ultracold mixtures of K and Cs and forming KCs molecules by magnetoassociation. We carry out coupled-channel calculations of the interspecies scattering length for ^{39}KCs, ^{41}KCs, and ^{40}KCs and characterize Feshbach resonances due to s-wave and d-wave bound states, with widths ranging from below 1 nG to 5 G. We also calculate the corresponding bound-state energies as a function of magnetic field. We give a general discussion of the combinations of intraspecies and interspecies scattering lengths needed to form low-temperature atomic mixtures and condensates and identify promising strategies for cooling and molecule formation for all three isotopic combinations of K and Cs.

DOI: 10.1103/PhysRevA.90.032716 PACS number(s): 34.50.Cx, 67.85.−d, 31.50.Bc, 34.20.Cf

I. INTRODUCTION

There is currently great interest in producing ultracold polar molecules [1,2]. Polar molecules can be oriented by electric fields and then have strongly anisotropic long-range interactions, which can produce a range of novel quantum phases and opportunities for quantum simulation and quantum information processing [3–5].

One way to produce ultracold molecules is by magnetoassociation of ultracold atoms followed by laser-induced transfer to a low-lying vibrational level. Pairs of atoms are first converted into "Feshbach molecules" in very high vibrational states by tuning an applied magnetic field across a zero-energy Feshbach resonance, and the molecules are then transferred into a low-lying level by stimulated Raman adiabatic passage (STIRAP). Ni *et al.* [6] have produced ^{40}K^{87}Rb molecules in their absolute ground state by this route. The ground-state KRb molecules can be transferred between hyperfine states using microwave radiation [7] and confined in one-dimensional [8] and three-dimensional [9] optical lattices. Nonpolar Cs_2 [10] and triplet Rb_2 [11] have been prepared using similar methods.

Many of the alkali-metal dimers, including KRb, can undergo exothermic bimolecular reactions to form pairs of homonuclear molecules. For fermionic ^{40}K^{87}Rb, these reactions are suppressed at very low temperatures for samples of molecules that are all in the same hyperfine level, but proceed very fast if more than one level is populated [12]. Even when suppressed, the reaction provides a loss mechanism for the ground-state molecules, and for bosonic molecules no suppression is expected. However, Żuchowski and Hutson [13] have shown that NaK, NaRb, NaCs, KCs, and RbCs are energetically stable to all possible two-body reactions. There is therefore particular interest in forming ultracold polar molecules of these species. Formation of Feshbach molecules has now been achieved for ^{23}Na^{40}K [14] and ^{87}RbCs [15,16]. Takekoshi *et al.* [17] have recently succeeded in producing around 1500 ^{87}RbCs molecules in their rovibrational ground state by magnetoassociation followed by STIRAP.

The purpose of the present paper is to investigate the feasibility of producing KCs molecules by magnetoassociation. KCs is of particular interest because it is predicted to have a dipole moment of 1.92 D [18], which is about 50% larger than RbCs; this allows dipolar interactions to dominate van der Waals interactions at lower electric fields and will make it easier to suppress collisions that sample short-range effects in quasi-two-dimensional geometries [19]. Interaction potentials for the lowest singlet and triplet states of KCs have been obtained by Ferber *et al.* [20], by fitting to extensive electronic spectra in a heat pipe [20,21], and have recently been refined to include coupled levels nearer dissociation [22]. Ferber *et al.* [20,22] carried out scattering calculations to identify Feshbach resonances in an s-only basis set (limited to functions with $L = 0$, where L is the end-over-end angular momentum of the two atoms about one another). However, for both RbCs and Cs_2, the resonances that have been used for molecule production arise from bound states with $L = 2$ (or higher for Cs_2). In the present work, we therefore carry out scattering and bound-state calculations including $L = 2$ functions, in order to understand the full range of possibilities. We then give a general discussion of the combinations of intraspecies and interspecies scattering lengths needed to form low-temperature atomic mixtures and condensates, and we examine the scattering properties to identify promising strategies for cooling and molecule formation for all three isotopic combinations of K and Cs.

II. THEORETICAL AND COMPUTATIONAL METHODS

The Hamiltonian for the interaction of two alkali-metal atoms in their ground ^2S states may be written as

$$\frac{\hbar^2}{2\mu}\left[-R^{-1}\frac{d^2}{dR^2}R+\frac{\hat{L}^2}{R^2}\right]+\hat{h}_1+\hat{h}_2+\hat{V}(R), \qquad (1)$$

where $\hat{L}^2$ is the operator for the end-over-end angular momentum of the two atoms about one another; $\hat{h}_1$ and $\hat{h}_2$ are the monomer Hamiltonians, including hyperfine couplings and Zeeman terms; and $\hat{V}(R)$ is the interaction operator.

In the present work we solve the scattering and bound-state problems by coupled-channels calculations using the MOLSCAT [23] and BOUND [24] packages, as modified to handle magnetic fields [25]. Both scattering and bound-state calculations use propagation methods and do not rely on basis sets in the interatomic distance coordinate R. The methodology

is exactly the same as that described for Cs in Sec. IV of Ref. [26] and so will not be repeated here. The calculations are performed using a fully uncoupled basis set,

$$|s_1 m_{s1}\rangle|i_1 m_{i1}\rangle|s_2 m_{s2}\rangle|i_2 m_{i2}\rangle|L M_L\rangle, \tag{2}$$

symmetrized for exchange symmetry when the two atoms are identical. s and i are the electron and nuclear spins, respectively. ^{39}K and ^{41}K have $i = 3/2$, while ^{40}K has $i = 4$ and an inverted hyperfine structure. The matrix elements of the different terms in the Hamiltonian in this basis set are given in the Appendix of Ref. [27]. The only rigorously conserved quantities are the parity, $(-1)^L$, and the projection of the total angular momentum, $M_{\rm tot} = M_F + M_L$, where $M_F = m_{s1} + m_{i1} + m_{s2} + m_{i2}$. M_F itself is nearly conserved except near avoided crossings. The basis sets include all functions for $L = 0$ and $L = 2$ with the required $M_{\rm tot}$.

The energy-dependent s-wave scattering length $a(k)$ is obtained from the diagonal S-matrix element in the incoming channel,

$$a(k) = \frac{1}{ik}\left(\frac{1 - S_{00}}{1 + S_{00}}\right), \tag{3}$$

where $k^2 = 2\mu E/\hbar^2$ and E is the kinetic energy [28]. Feshbach resonances are initially located using the FIELD package [29], which provides a complete list of the magnetic fields at which bound states cross a threshold (or cross a specified energy). The resonances are then characterized by running MOLSCAT at fields close to resonance and converging numerically on the pole position using the formula [30]

$$a(B) = a_{\rm bg}\left(1 - \frac{\Delta}{B - B_0}\right), \tag{4}$$

where B_0 is the resonance position and Δ is its width. This procedure is able to locate and characterize resonances with widths as small as a few pG.

The interaction operator $\hat{V}(R)$ may be written as

$$\hat{V}(R) = \hat{V}^{\rm c}(R) + \hat{V}^{\rm d}(R). \tag{5}$$

Here $\hat{V}^{\rm c}(R) = V_0(R)\hat{\mathcal{P}}^{(0)} + V_1(R)\hat{\mathcal{P}}^{(1)}$ is an isotropic potential operator that depends on the electronic potential energy curves $V_0(R)$ and $V_1(R)$ for the lowest singlet and triplet states of KCs. The singlet and triplet projectors $\hat{\mathcal{P}}^{(0)}$ and $\hat{\mathcal{P}}^{(1)}$ project onto subspaces with total electron spin quantum numbers of 0 and 1, respectively. The potential curves for the singlet and triplet states of KCs are taken from Ferber *et al.* [22]. These curves are expected to produce resonance positions with an absolute uncertainty of 5 to 10 G, with considerably lower uncertainties in the relative positions. The potentials for K_2 were taken from Falke *et al.* [31], while the Cs intraspecies scattering length was taken from the tabulation of Berninger *et al.* [26].

At long range, the coupling $\hat{V}^{\rm d}(R)$ of Eq. (5) has a simple magnetic dipole-dipole form that varies as $1/R^3$ [30,32]. However, for heavy atoms it is known that second-order spin-orbit coupling provides an additional contribution that has the same tensor form as the dipole-dipole term. This contribution dominates at short range for species containing Cs [33,34] and has a large effect on the widths of resonances due to states with $L > 0$. In the present work, $\hat{V}^{\rm d}(R)$ is represented as

$$\hat{V}^{\rm d}(R) = \lambda(R)[\hat{s}_1 \cdot \hat{s}_2 - 3(\hat{s}_1 \cdot \vec{e}_R)(\hat{s}_2 \cdot \vec{e}_R)], \tag{6}$$

where $\vec{e}_R$ is a unit vector along the internuclear axis and λ is an R-dependent coupling constant. For both Cs_2 [34] and RbCs [15], electronic structure calculations showed that the second-order spin-orbit splitting can be represented by a biexponential form, so that the overall form of $\lambda(R)$ is

$$\lambda(R) = E_{\rm h}\alpha^2\left\{A_{\rm 2SO}^{\rm short}\exp\left[-\beta_{\rm 2SO}^{\rm short}(R/a_0)\right] + A_{\rm 2SO}^{\rm long}\exp\left[-\beta_{\rm 2SO}^{\rm long}(R/a_0)\right] + \frac{1}{(R/a_0)^3}\right\}, \tag{7}$$

where $\alpha \approx 1/137$ is the atomic fine-structure constant and a_0 is the Bohr radius. The second-order spin-orbit coupling has not been calculated for KCs, but an estimate may be made from the values for Cs_2 and RbCs. It is physically reasonable to suppose that the coupling comes principally from the Cs atom(s) and (for chemically similar species) does not depend strongly on the identity of the other atom. Evaluating the second-order spin-orbit contribution to $\lambda(R)$ [15,34] at the inner turning point of the triplet curve at zero energy gives values per Cs atom within about 40% of one another for Cs_2 and RbCs. In the present work, we simply shifted the RbCs function inwards 0.125 a_0, to give the same value at the inner turning point for KCs as for RbCs. We thus use $\beta_{\rm 2SO}^{\rm short} = 0.80$ and $\beta_{\rm 2SO}^{\rm long} = 0.28$, as for RbCs [15], with $A_{\rm 2SO}^{\rm short} = -45.5$ and $A_{\rm 2SO}^{\rm long} = -0.032$.

III. RESULTS

A. ^{39}KCs

Figure 1 shows the scattering length and the corresponding near-threshold bound states for ^{39}KCs. When only s-wave basis functions are included [Fig. 1(a)], the scattering length shows 5 resonances below 1000 G, where s-wave bound states [black in Fig. 1(d)] cross the lowest threshold. These agree within 1 G with those calculated by Ferber *et al.* [22]. When d-wave ($L = 2$) basis functions are included, an additional 30 bound states cross the threshold below 1000 G. These are color-coded according to M_F in Fig. 1(d). If only the long-range spin-spin coupling is included [the R^{-3} term in Eq. (7)], the resonances due to d-wave states are quite narrow [Fig. 1(b)]. However, if second-order spin-orbit coupling is included, most of them become significantly broader, as shown in Fig. 1(c) (note the logarithmic scale of the vertical bars used to indicate the resonance widths). Some of the resonances have widths suitable for use in molecule formation. The positions and widths of some of the broader resonances are given in Table I, and a complete tabulation (all resonances, with and without second-order spin-orbit coupling for ^{39}KCs) is included in the Supplemental Material [35].

It is clearly important to include second-order spin-orbit coupling in calculations involving heavy atoms such as Cs. In the following sections, only calculations including the second-order spin-orbit coupling are presented.

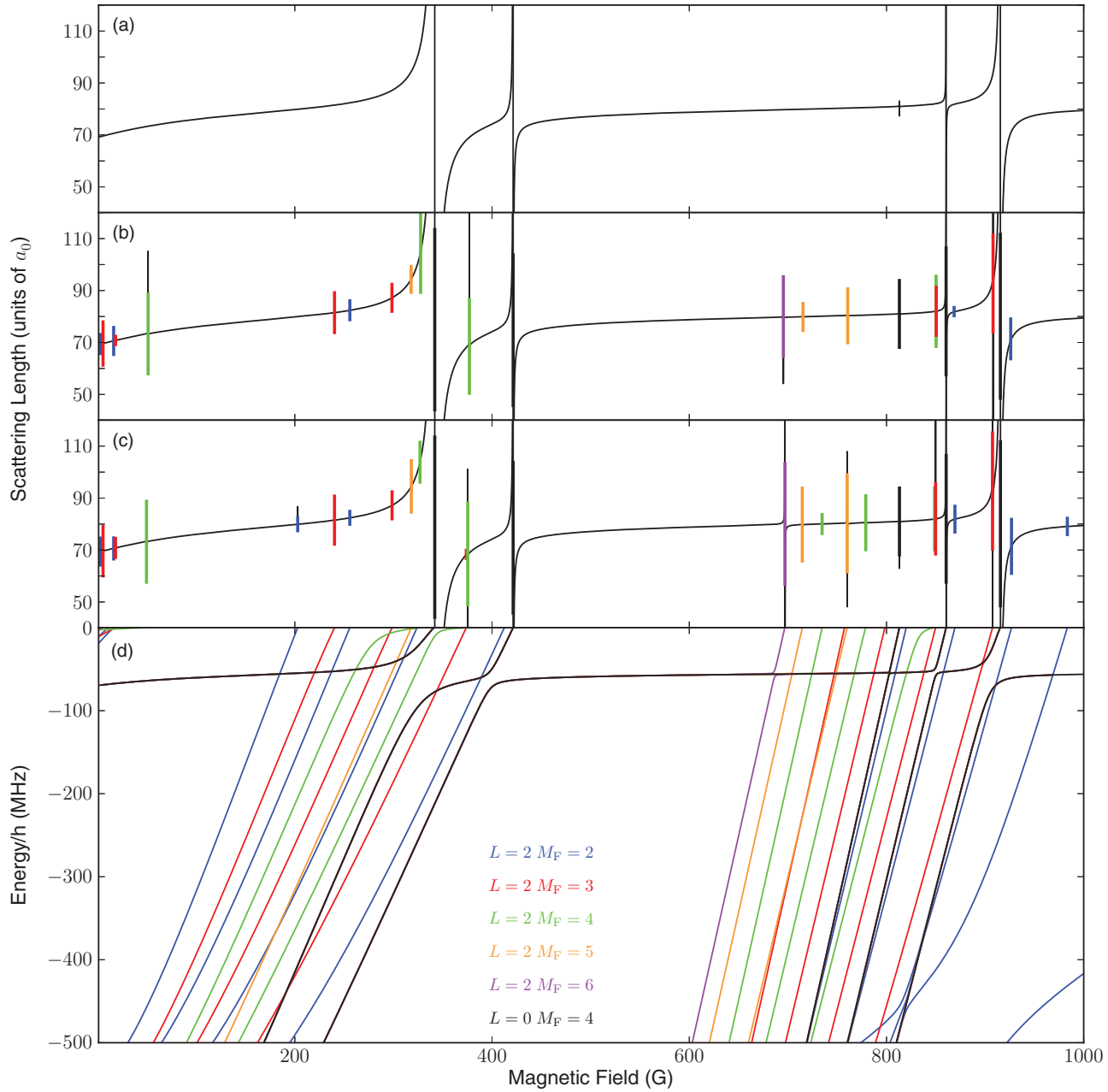

FIG. 1. (Color online) $^{39}K^{133}Cs$: (a) scattering length with $L = 0$ functions only; (b) scattering length with $L = 0$ and 2 functions, but second-order spin-orbit coupling not included; (c) scattering length with $L = 0$ and 2 functions, and approximate model of second-order spin-orbit coupling included; and (d) bound states. Resonance widths greater than 1 μG are shown as vertical bars with lengths proportional to $\log_{10} \Delta/\mu$G.

B. ^{41}KCs

Figure 2 shows the scattering length and the corresponding near-threshold bound states for ^{41}KCs. In this case there is an s-wave bound state only about 3 MHz $\times$ h below threshold, which produces a background scattering length that is large and positive (though not so large as for ^{87}RbCs and Cs_2). There are 7 resonances below 1000 G due to s-wave states; it may be noted that Ferber *et al.* [20] were able to locate only 6 of these. In addition, the rich set of d-wave levels produces 24 resonances below about 130 G, some of which offer good prospects for molecule formation, as discussed below.

C. ^{40}KCs

Figure 3 shows the scattering length and the corresponding near-threshold bound states for ^{40}KCs. In this case there is a very dense bound-state spectrum, with 14 s-wave levels and a further 70 d-wave levels crossing the threshold below 1000 G. However, the resulting resonances are all quite weak (note the contracted vertical scale of Fig. 3). Indeed, Ferber *et al.* [20] located only the 2 broadest resonances, although they commented that a further 13 s-wave resonances should exist. The widest d-wave resonance has $\Delta \approx 10$ mG, and many have $\Delta < 1$ nG. The narrowness arises because the singlet and triplet scattering lengths are quite similar, which directly

TABLE I. Listing of all s-wave Feshbach resonances and d-wave Feshbach resonances with widths over 1 mG for all isotopes of KCs in the field range 0 to 1000 G. A complete tabulation of all resonances is included in the Supplemental Material [35].

B_0 (G)	Δ (G)	a_{bg} (a_0)	L	M_F
		^{39}KCs		
49.57	0.001	73.2	2	4
341.90	4.8	79.0	0	4
375.35	0.006	68.5	2	4
421.36	0.4	74.7	0	4
697.02	0.03	80.0	2	6
760.13	0.004	80.3	2	5
813.14	3×10^{-4}	81.0	0	4
860.52	0.05	82.0	0	4
907.54	0.02	92.7	2	3
915.56	1.2	80.1	0	4
		^{40}KCs		
57.59	$<10^{-9}$	−40.3	0	−3/2
69.85	$<10^{-9}$	−40.3	0	−3/2
89.01	$<10^{-9}$	−40.3	0	−3/2
122.77	$<10^{-9}$	−40.3	0	−3/2
192.18	−0.001	−40.2	2	−3/2
196.71	-3×10^{-7}	−40.2	0	−3/2
215.96	−0.01	−40.2	2	−1/2
230.24	$<10^{-9}$	−40.2	0	−3/2
234.15	$<10^{-9}$	−40.1	0	−3/2
239.55	$<10^{-9}$	−40.1	0	−3/2
246.44	-4×10^{-7}	−40.0	0	−3/2
254.52	-1×10^{-4}	−39.8	0	−3/2
264.34	−0.1	−40.3	0	−3/2
379.60	−0.002	−40.3	2	−5/2
470.25	−0.01	−40.2	0	−3/2
677.44	$<10^{-9}$	−40.2	0	−3/2
902.84	$<10^{-9}$	−40.2	0	−3/2
		^{41}KCs		
23.89	0.02	193.0	2	6
25.68	0.03	189.3	2	5
28.41	0.007	188.7	2	4
87.38	0.003	201.6	2	4
90.10	0.008	201.1	2	5
94.28	0.001	201.5	2	3
109.86	0.002	204.5	2	2
120.89	0.02	206.0	0	4
168.19	0.6	262.6	0	4
171.20	1.2	151.3	0	4
861.03	0.03	247.7	2	5
884.92	4.1	211.4	0	4
966.89	0.1	201.5	0	4

reduces the strength of the resonances due to s-wave states [36] and indirectly reduces the strength of those due to d-wave states as well.

IV. PROSPECTS FOR PRODUCING KCs MOLECULES

We now discuss the implications of the predicted scattering lengths and interspecies Feshbach resonances for the formation of mixtures of ultracold K and Cs and the production of ultracold KCs molecules. We begin with a general discussion of the scattering properties required and then proceed to consider their implications for the isotopologs of KCs.

It should be noted that the remaining uncertainties in the KCs potential curves of Ref. [22] may shift the interspecies resonances by a few Gauss and may thus change the quantitative predictions in some cases, but the overall picture is robust. Once resonance positions are observed for one isotopic combination, it will be possible to refine the potentials and improve the detailed predictions.

A. General considerations

Magnetoassociation has been demonstrated in a wide range of atomic systems, using resonances with widths varying from a few mG to over 10 G [37]. The wider resonances allow slower magnetic field ramp speeds while maintaining adiabaticity through the avoided crossing between atomic and molecular states. However, dwelling too long near the pole of the resonance can lead to enhanced three-body losses and in practice the speed of the magnetic field ramp has to be carefully optimized. The overall conversion efficiency is dictated by the phase-space density of the atomic gas. Magnetoassociation can be carried out in a thermal gas close to degeneracy [38], but it is best performed in the quantum-degenerate regime; this produces a molecular gas that is colder and has higher phase-space density, and so is more suitable for experiments that aim for quantum coherence.

The need to produce an atomic gas close to quantum degeneracy for magnetoassociation requires the ratio of "good" (elastic) to "bad" (inelastic and three-body loss) collisions to be suitable for efficient evaporative cooling [39,40]. While loss rates vary considerably from one species to another, it is generally observed in single-species experiments that the evaporation is most efficient if the s-wave scattering length a satisfies $40\ a_0 \lesssim |a| \lesssim 250\ a_0$ [41–44]. Below this range the elastic collision rate (which scales as a^2 in the ultracold limit) becomes too low for cooling to proceed efficiently [45], and above it the three-body loss rate (which scales as a^4 [49]) becomes too high. For species where the background scattering length falls outside this range, magnetic tuning of the scattering length near Feshbach resonances has proved an essential tool to reach quantum degeneracy [50–53]. In such cases, the inelastic and three-body loss rates also tune with the magnetic field [54] allowing the ratio of elastic collisions to those causing loss to be optimized [55]. In some cases, most notably Cs, the a^4 scaling of the three-body loss rate is significantly modified by the Efimov effect [56,57], allowing particularly efficient evaporative cooling around the resulting three-body recombination minimum [26,58,59].

In the case of an atomic mixture, the need to cool both species to high phase-space densities puts conditions on both the intraspecies scattering lengths (hereafter a_{11} and a_{22}) and the interspecies scattering length (a_{12}). There are several different scenarios that can produce efficient cooling. If a_{11} and a_{12} are in the desired range, species 1 can be cooled directly and species 2 will be cooled by interspecies collisions [60–65]. In this case the only restriction on a_{22} is that its magnitude should not be so large as to produce unacceptable three-body loss. This typically restricts $|a_{22}|$ to values below about 600 a_0. Alternatively, if a_{11} and a_{22} are in the desired range but

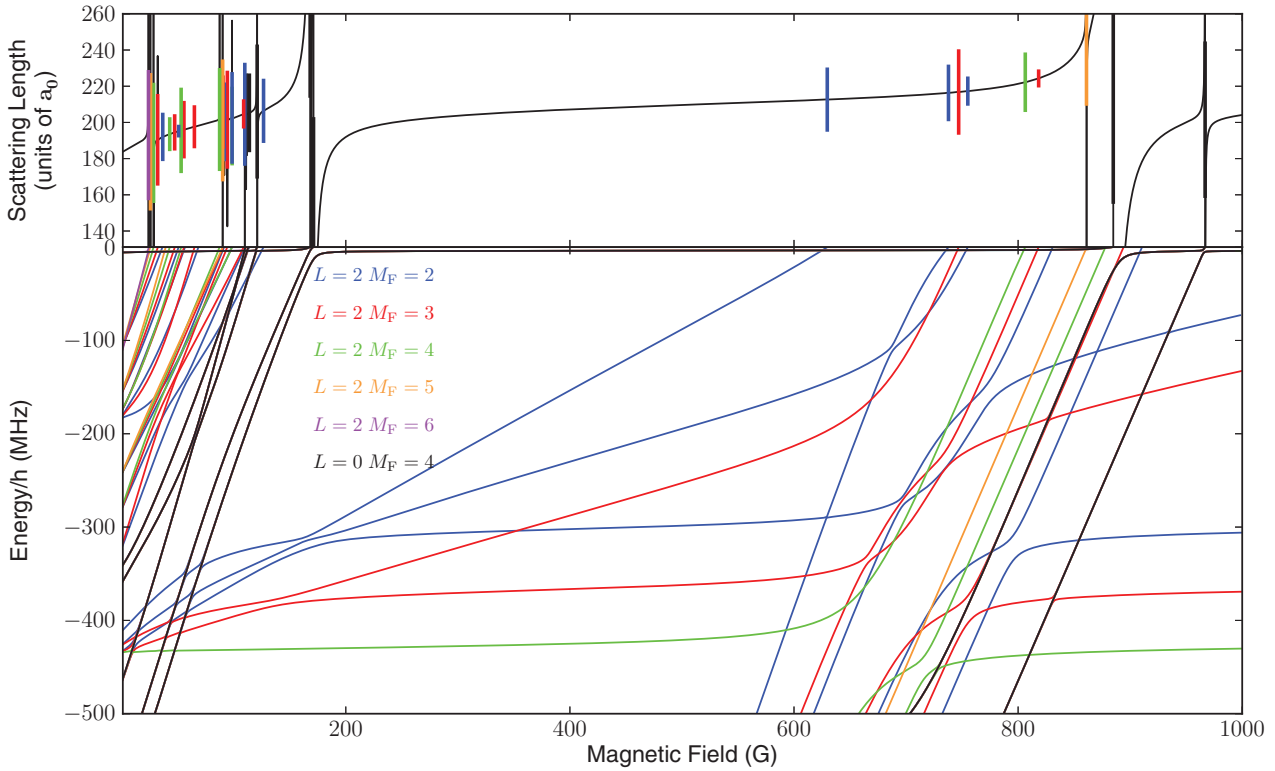

FIG. 2. (Color online) $^{41}K^{133}Cs$: (a) scattering length with $L = 0$ and 2 functions, and approximate model of second-order spin-orbit coupling; and (b) bound states. Resonance widths greater than 1 μG are shown as vertical bars with lengths proportional to $\log_{10} \Delta/\mu G$, on the same scale as in Fig. 1.

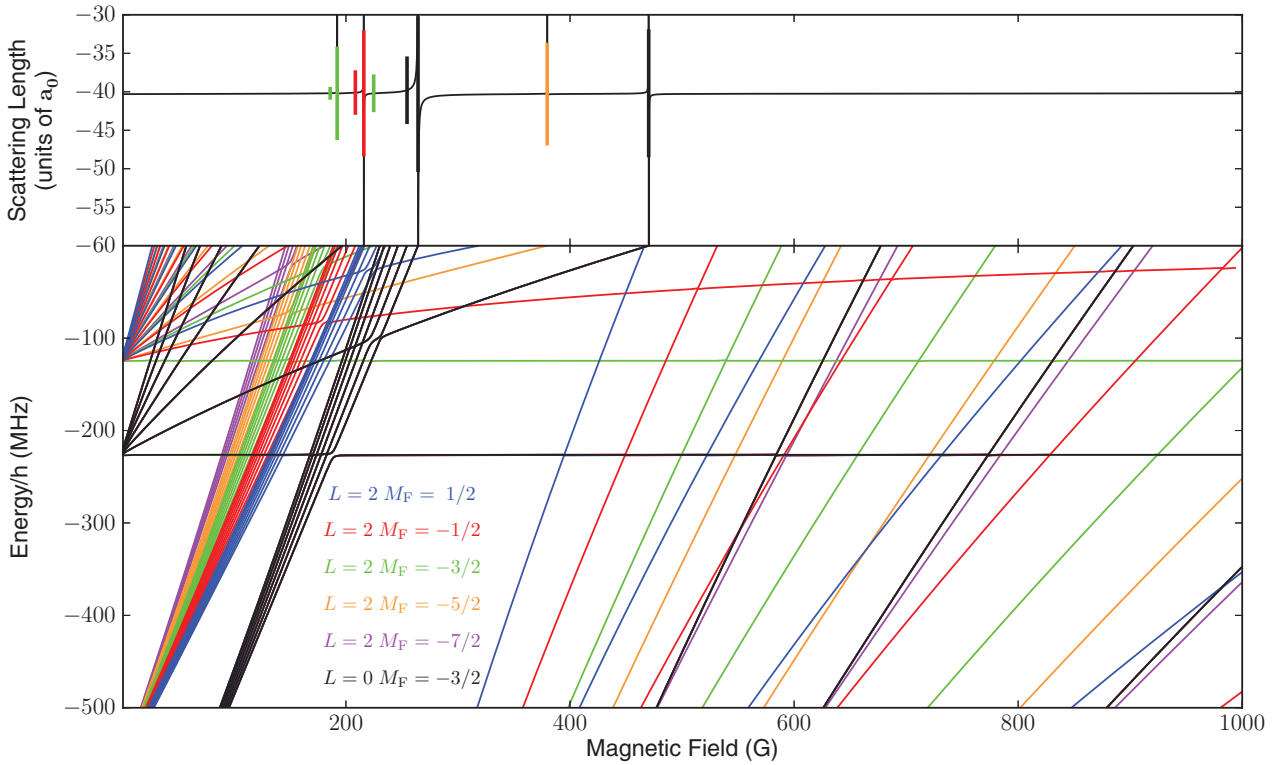

FIG. 3. (Color online) $^{40}K^{133}Cs$: (a) scattering length with $L = 0$ and 2 functions, and approximate model of second-order spin-orbit coupling; and (b) bound states. Resonance widths greater than 1 μG are shown as vertical bars with lengths proportional to $\log_{10} \Delta/\mu G$, on the same scale as in Fig. 1.

a_{12} is not, the two species can be cooled independently, either in the same trap (if $|a_{12}|$ is small [66]) or separately (if $|a_{12}|$ is large [15]). In the latter case it is necessary to overlap the clouds in a subsequent step. If none of the above scenarios can be realized for atoms in their absolute ground states, it may be possible to cool one or both species in an excited Zeeman or hyperfine state, although this introduces the possibility of further loss via two-body inelastic collisions. Finally, if the desired conditions cannot be fulfilled at a single magnetic field, it might be feasible to cool the two species in separate traps at different fields, though this would introduce substantial extra complexity.

If cooling proceeds all the way to Bose-Einstein condensation, there are further restrictions. Large individual condensates are stable with respect to collapse only if $a_{11} > 0$ and $a_{22} > 0$, and the mixed condensate requires in addition that $g_{12}^2 < g_{11}g_{22}$, where the interaction coupling constants are [67]

$$g_{ij} = 2\pi\hbar^2 a_{ij}\left(\frac{m_i + m_j}{m_i m_j}\right). \tag{8}$$

If g_{12} is too positive, the mean-field repulsion leads to phase separation, whereas if it is too negative the mixed condensate collapses. However, the magnetic field at which the condensates are mixed need not be the same as the one used for the early stages of evaporative or sympathetic cooling [16]. The instabilities can also, in principle, be avoided by loading the two species into a three-dimensional optical lattice prior to molecule formation to realize a Mott-insulator phase with exactly one atom of each species per lattice site [68].

Magnetoassociation can in principle be carried out at a field different from that used to form the atomic mixture. However, the mixture must be stable for the duration of the magnetoassociation sequence, which is typically a few milliseconds. For a mixed condensate, the stability conditions are those given above. For a thermal gas close to degeneracy, the conditions are less restrictive but magnetoassociation is less efficient.

B. Implications for KCs

Figure 4 shows the intraspecies and interspecies scattering lengths for all the atoms important for KCs molecule formation, together with the positions of interspecies resonances. The colored bars below each interspecies scattering length show the fields at which both species can be cooled evaporatively (red, top), the fields at which one species can be cooled evaporatively and the other sympathetically (blue, center), and the fields at which the condensates are stable and miscible (green, bottom).

The intraspecies scattering length for Cs is shown in Fig. 4(a). The large background value places severe limitations on the magnetic fields where efficient evaporative cooling is possible. Bose-Einstein condensates of Cs have been produced only in the $f = 3$, $m_f = 3$ ground state, where two-body inelastic collisions cannot occur. Even in this state, the magnetic field used for cooling must be chosen to tune the scattering length to a moderate positive value to prevent excessive three-body losses. Condensates of Cs are usually produced at fields around 21 G [52,69,70], just above the zero crossing in the scattering length at 17 G. Similar windows of moderate positive scattering lengths exist above zero crossings at 556 and 881 G, associated with broad Feshbach resonances at 549 and 787 G; Berninger *et al.* [26] carried out cooling at 558.7 and 894 G, where three-body losses are low [59]. Table II summarizes the intraspecies and interspecies scattering lengths at the boundaries of the regions of moderate positive Cs scattering length.

The intraspecies scattering length for ^{39}K is shown in Fig. 4(b). It varies weakly with magnetic field and is generally small and negative except near the Feshbach resonance at 402 G. The small value limits the rate of rethermalization and the negative sign makes a single-species condensate of ^{39}K unstable at most fields. These hurdles have been overcome to produce condensates in the $f = 1$, $m_f = 1$ ground state by using a combination of sympathetic cooling with ^{87}Rb and Feshbach tuning of the ^{39}K scattering length [71]. More recently, direct evaporation of ^{39}K to condensation has been achieved using several different Feshbach resonances, including the one at 402 G in the ground state [53]. The interspecies scattering length for ^{39}KCs shown is shown in Fig. 4(c); at 21 G it is approximately $+70\ a_0$, which may allow sympathetic cooling of ^{39}K by Cs. The situation is similar at 558.7 and 894 G. For ^{39}KCs, most of the resonances that are broad enough for magnetoassociation lie above 300 G, at fields where the ^{39}K intraspecies scattering length is negative. The Cs intraspecies scattering length is very large at most ^{39}KCs resonances that lie below the Cs pole at 787 G, but crosses zero near 881 G [26] and has more moderate values at fields around the zero crossing. The most promising ^{39}KCs resonances for magnetoassociation in a thermal gas are therefore those at 861, 908, and 916 G, where the Cs scattering length is calculated to be -630, 510, and 630 bohr, respectively. There is also a region from 353 to 402 G, where the condensates are predicted to be stable and miscible. The resonance at 375 G ($\Delta = 6$ mG) is very promising for magnetoassociation to form ^{39}KCs in a mixed condensate. Just below 353 G, the ^{39}K intraspecies scattering length is small and negative, but it has reached only $-4\ a_0$ at the ^{39}KCs resonance at 342 G ($\Delta = 4.8$ G). It may therefore be possible to sweep the magnetic field across this resonance to perform magnetoassociation before the condensate has time to collapse. The Cs intraspecies scattering length is very large at these resonances ($2540\ a_0$ at 375 G and $2420\ a_0$ at 342 G [26]), but magnetoassociation to form ^{87}RbCs has been achieved in a thermal gas [15–17] at a resonance at 197.1 G, where the Cs scattering length is $1970\ a_0$ [26], and three-body collisions are suppressed by a factor of 6 in a condensate [72] compared to a thermal gas.

The intraspecies scattering length for ^{41}K is shown in Fig. 4(d). By contrast to ^{39}K, it varies only slightly from a background value of approximately $+63\ a_0$. Direct evaporation to Bose-Einstein condensation has been achieved in the magnetically trappable $f = 2$, $m_f = 2$ excited state [44], where the scattering length is $+61\ a_0$ [31]. Efficient evaporation is also expected for atoms in the $f = 1$, $m_f = 1$ ground state confined in an optical dipole trap. The interspecies scattering length for ^{41}KCs is shown in Fig. 4(e); at 21 G it is approximately $200\ a_0$, which will lead to rapid interspecies thermalization and may allow ^{41}K to be used as a sympathetic coolant for Cs following the approach used with ^{87}Rb [70].

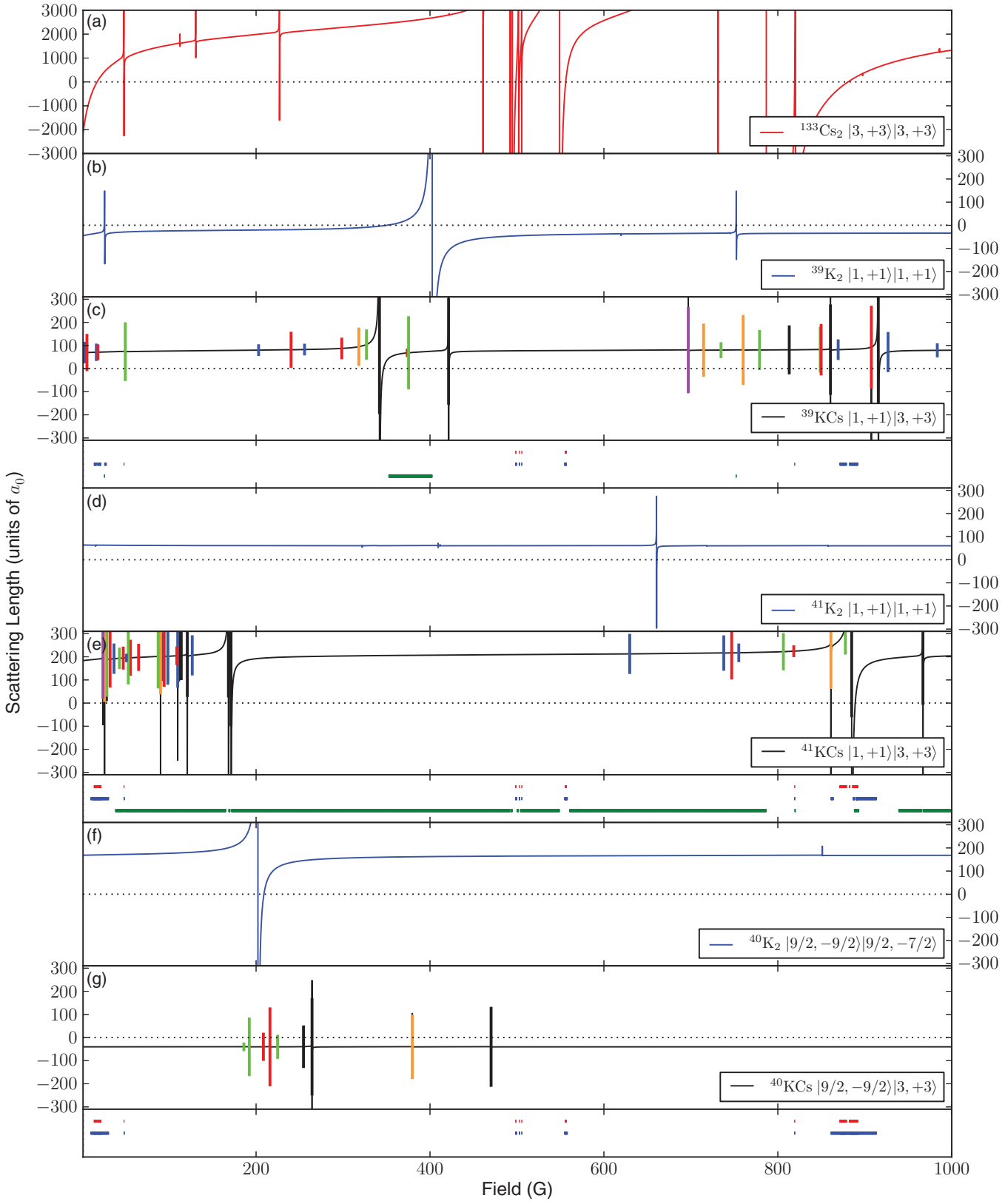

FIG. 4. (Color online) Scattering lengths for isotopologs of KCs, together with those of the corresponding isotopes of K and Cs. The scattering lengths are shown with the same magnetic field axis to facilitate the identification of regions where the combination is conducive to molecule formation. Resonance widths greater than 1 μG are shown as vertical bars with lengths proportional to $\log_{10} \Delta/\mu$G. The colored bars beneath each interspecies scattering length indicate the fields at which both species can be cooled evaporatively (red, top), the fields at which one species can be cooled evaporatively and the other sympathetically (blue, center), and the fields at which the condensates are stable and miscible (green, bottom, not shown for ^{40}K).

TABLE II. Intraspecies and interspecies scattering lengths at fields that bound the regions where 40 $a_0 \lesssim a_{Cs} \lesssim 250\ a_0$.

	Scattering length (a_0)						
Field (G)	^{133}Cs	^{39}K	^{39}KCs	^{41}K	^{41}KCs	^{40}K	^{40}KCs
17.7	35.2	−34.0	70.8	63.1	189.6	169.6	−40.3
21.7	252.5	−30.7	71.1	62.9	192.2	169.9	−40.3
556.2	28.2	−40.0	78.2	60.5	210.9	165.7	−40.3
556.9	253.6	−40.0	78.2	60.5	210.9	165.8	−40.3
882.3	39.3	−34.5	83.1	60.3	539.9[a]	167.8	−40.2
892.2	251.3	−34.5	84.5	60.3	93.2[a]	167.8	−40.2

[a]^{41}KCs has a resonance at 884.9 G that substantially affects its scattering length in this region.

The situation is similar around 558.7 and 894 G. At all these fields, the combination of a moderately large interspecies scattering length and a relatively low Cs scattering length will produce phase separation if the mixture is cooled to degeneracy. However, in all cases there are nearby fields where a larger Cs scattering length makes the condensates miscible. ^{41}KCs has a rich spectrum of usable resonances, including 10 resonances below 200 G. In particular, there are 3 resonances below 30 G which lie close to a region where efficient evaporative cooling of both species is possible. These are comparable in width to the Cs resonance at 19.8 G that has been used extensively in the creation and study of ultracold Cs_2 molecules [73–75]. Since the combination of scattering lengths at these fields will lead to phase separation, these resonances would need to be accessed in thermal gases. However, the condensates are expected to be miscible at most fields between 38 and 786 G and above 939 G, and there are several resonances in these regions that are promising for magnetoassociation in a mixed condensate. There is also a small region of miscibility (5 G wide) immediately above the broad ^{41}KCs resonance at 885 G ($\Delta = 4.1$ G), where a_K is 63 a_0 and a_{Cs} is around 200 a_0. This combination of properties is very promising for cooling a mixed gas directly to degeneracy, followed by magnetoassociation.

The s-wave scattering length is undefined for two ^{40}K atoms in identical states because of their fermionic character. Because of this, ^{40}K is usually cooled by interspecies collisions between atoms in different Zeeman states [76]. The scattering length for collisions between atoms in the $f = 9/2, m_f = -9/2$ and $f = 9/2, m_f = -7/2$ states is shown in Fig. 4(f). It varies weakly with magnetic field and is generally around +170 a_0 except near the Feshbach resonance at 202 G. The interspecies scattering length for ^{40}KCs is approximately −40 a_0 at nearly all fields. It may therefore be possible to use sympathetic cooling of ^{40}K with Cs, in one of the regions where Cs itself can be cooled, to avoid the need for two different spin states of ^{40}K. As discussed above, most of the resonances for ^{40}KCs are exceedingly narrow. However, resonances that may be suitable for the production of fermionic molecules are predicted to exist at 192, 216, 264, and 470 G.

V. CONCLUSIONS

We have explored the possibilities for magnetoassociation to form ultracold KCs molecules, using calculations of bound states and scattering properties. We have calculated the interspecies scattering length for ^{39}KCs, ^{41}KCs, and ^{40}KCs. We have characterized Feshbach resonances in s-wave scattering due to s-wave and d-wave bound states, with widths ranging from below 1 nG to 5 G, and we have carried out bound-state calculations to identify the quantum states responsible.

We have considered the combinations of intraspecies and interspecies scattering lengths to identify possibilities for producing both mixed condensates and low-temperature thermal mixtures of K and Cs. All the isotopic combinations offer promising possibilities for producing mixtures with high phase-space densities and for magnetoassociation to form Feshbach molecules.

Our calculations of interspecies scattering lengths are based on the singlet and triplet potential curves of Ref. [22]. Remaining uncertainties in the potential curves result in uncertainties of at least a few gauss in the predicted resonance positions. Once the actual positions of interspecies Feshbach resonances have been measured and assigned for at least one isotopolog of KCs, it will be possible to refine the potentials to make more accurate predictions of the scattering properties.

ACKNOWLEDGMENTS

The authors acknowledge the support of the Engineering and Physical Sciences Research Council (Grant No. EP/I012044/1) and the European Office of Aerospace Research and Development (Grant No. FA8655-10-1-3033). C.L.B. is supported by a Doctoral Fellowship from Durham University.

[1] L. D. Carr, D. DeMille, R. V. Krems, and J. Ye, New J. Phys. **11**, 055049 (2009).
[2] B. Friedrich and J. M. Doyle, Chem. Phys. Chem **10**, 604 (2009).
[3] B. Capogrosso-Sansone, C. Trefzger, M. Lewenstein, P. Zoller, and G. Pupillo, Phys. Rev. Lett. **104**, 125301 (2010).
[4] A. Micheli, G. Pupillo, H. P. Büchler, and P. Zoller, Phys. Rev. A **76**, 043604 (2007).
[5] M. L. Wall and L. D. Carr, New J. Phys. **11**, 055027 (2009).
[6] K.-K. Ni, S. Ospelkaus, M. H. G. de Miranda, A. Pe'er, B. Neyenhuis, J. J. Zirbel, S. Kotochigova, P. S. Julienne, D. S. Jin, and J. Ye, Science **322**, 231 (2008).
[7] S. Ospelkaus, K.-K. Ni, G. Quéméner, B. Neyenhuis, D. Wang, M. H. G. de Miranda, J. L. Bohn, J. Ye, and D. S. Jin, Phys. Rev. Lett. **104**, 030402 (2010).
[8] M. H. G. de Miranda, A. Chotia, B. Neyenhuis, D. Wang, G. Quéméner, S. Ospelkaus, J. L. Bohn, J. Ye, and D. S. Jin, Nat. Phys. **7**, 502 (2011).

[9] A. Chotia, B. Neyenhuis, S. A. Moses, B. Yan, J. P. Covey, M. Foss-Feig, A. M. Rey, D. S. Jin, and J. Ye, Phys. Rev. Lett. **108**, 080405 (2012).

[10] J. G. Danzl, M. J. Mark, E. Haller, M. Gustavsson, R. Hart, J. Aldegunde, J. M. Hutson, and H.-C. Nägerl, Nat. Phys. **6**, 265 (2010).

[11] F. Lang, K. Winkler, C. Strauss, R. Grimm, and J. Hecker Denschlag, Phys. Rev. Lett. **101**, 133005 (2008).

[12] S. Ospelkaus, K.-K. Ni, D. Wang, M. H. G. de Miranda, B. Neyenhuis, G. Quéméner, P. S. Julienne, J. L. Bohn, D. S. Jin, and J. Ye, Science **327**, 853 (2010).

[13] P. S. Żuchowski and J. M. Hutson, Phys. Rev. A **81**, 060703(R) (2010).

[14] C.-H. Wu, J. W. Park, P. Ahmadi, S. Will, and M. W. Zwierlein, Phys. Rev. Lett. **109**, 085301 (2012).

[15] T. Takekoshi, M. Debatin, R. Rameshan, F. Ferlaino, R. Grimm, H.-C. Nägerl, C. R. Le Sueur, J. M. Hutson, P. S. Julienne, S. Kotochigova, and E. Tiemann, Phys. Rev. A **85**, 032506 (2012).

[16] M. P. Köppinger, D. J. McCarron, D. L. Jenkin, P. K. Molony, H.-W. Cho, S. L. Cornish, C. R. Le Sueur, C. L. Blackley, and J. M. Hutson, Phys. Rev. A **89**, 033604 (2014).

[17] T. Takekoshi, L. Reichsöllner, A. Schindewolf, J. M. Hutson, C. R. Le Sueur, O. Dulieu, F. Ferlaino, R. Grimm, and H.-C. Nägerl, arXiv:1405.6037.

[18] M. Aymar and O. Dulieu, J. Chem. Phys. **122**, 204302 (2005).

[19] P. S. Julienne, T. M. Hanna, and Z. Idziaszek, Phys. Chem. Chem. Phys. **13**, 19114 (2011).

[20] R. Ferber, I. Klincare, O. Nikolayeva, M. Tamanis, H. Knöckel, E. Tiemann, and A. Pashov, Phys. Rev. A **80**, 062501 (2009).

[21] R. Ferber, I. Klincare, O. Nikolayeva, M. Tamanis, H. Knöckel, E. Tiemann, and A. Pashov, J. Chem. Phys. **128**, 244316 (2008).

[22] R. Ferber, O. Nikolayeva, M. Tamanis, H. Knöckel, and E. Tiemann, Phys. Rev. A **88**, 012516 (2013).

[23] J. M. Hutson and S. Green, MOLSCAT computer program, version 14, distributed by Collaborative Computational Project No. 6 of the UK Engineering and Physical Sciences Research Council (1994).

[24] J. M. Hutson, BOUND computer program, version 5, distributed by Collaborative Computational Project No. 6 of the UK Engineering and Physical Sciences Research Council (1993).

[25] M. L. González-Martínez and J. M. Hutson, Phys. Rev. A **75**, 022702 (2007).

[26] M. Berninger, A. Zenesini, B. Huang, W. Harm, H.-C. Nägerl, F. Ferlaino, R. Grimm, P. S. Julienne, and J. M. Hutson, Phys. Rev. A **87**, 032517 (2013).

[27] J. M. Hutson, E. Tiesinga, and P. S. Julienne, Phys. Rev. A **78**, 052703 (2008). Note that the matrix element of the dipolar spin-spin operator given in Eq. (A2) of this paper omits a factor of $-\sqrt{30}$.

[28] J. M. Hutson, New J. Phys. **9**, 152 (2007).

[29] J. M. Hutson, FIELD computer program, version 1 (2011).

[30] A. J. Moerdijk, B. J. Verhaar, and A. Axelsson, Phys. Rev. A **51**, 4852 (1995).

[31] S. Falke, H. Knöckel, J. Friebe, M. Riedmann, E. Tiemann, and C. Lisdat, Phys. Rev. A **78**, 012503 (2008).

[32] H. T. C. Stoof, J. M. V. A. Koelman, and B. J. Verhaar, Phys. Rev. B **38**, 4688 (1988).

[33] F. H. Mies, C. J. Williams, P. S. Julienne, and M. Krauss, J. Res. Natl. Inst. Stand. Technol. **101**, 521 (1996).

[34] S. Kotochigova, E. Tiesinga, and P. S. Julienne, Phys. Rev. A **63**, 012517 (2000).

[35] See Supplemental Material at http://link.aps.org/supplemental/10.1103/PhysRevA.90.032716 for a full listing of the resonance positions and widths.

[36] P. S. Julienne, F. H. Mies, E. Tiesinga, and C. J. Williams, Phys. Rev. Lett. **78**, 1880 (1997).

[37] C. Chin, R. Grimm, P. Julienne, and E. Tiesinga, Rev. Mod. Phys. **82**, 1225 (2010).

[38] E. Hodby, S. T. Thompson, C. A. Regal, M. Greiner, A. C. Wilson, D. S. Jin, E. A. Cornell, and C. E. Wieman, Phys. Rev. Lett. **94**, 120402 (2005).

[39] W. Ketterle and N. van Druten, Adv. At. Mol. Opt. Phys. **37**, 181 (1996).

[40] J. Weiner, V. S. Bagnato, S. Zilio, and P. S. Julienne, Rev. Mod. Phys. **71**, 1 (1999).

[41] M. H. Anderson, J. R. Ensher, M. R. Matthews, C. E. Wieman, and E. A. Cornell, Science **269**, 198 (1995).

[42] K. B. Davis, M. O. Mewes, M. R. Andrews, N. J. van Druten, D. S. Durfee, D. M. Kurn, and W. Ketterle, Phys. Rev. Lett. **75**, 3969 (1995).

[43] Y. Takasu, K. Maki, K. Komori, T. Takano, K. Honda, M. Kumakura, T. Yabuzaki, and Y. Takahashi, Phys. Rev. Lett. **91**, 040404 (2003).

[44] T. Kishimoto, J. Kobayashi, K. Noda, K. Aikawa, M. Ueda, and S. Inouye, Phys. Rev. A **79**, 031602 (2009).

[45] For lighter species such as ^{7}Li [46] and metastable He [47, 48], slightly smaller scattering lengths can be used because of the inverse scaling of the collision rate with mass.

[46] C. C. Bradley, C. A. Sackett, and R. G. Hulet, Phys. Rev. Lett. **78**, 985 (1997).

[47] A. Robert, O. Sirjean, A. Browaeys, J. Poupard, S. Nowak, D. Boiron, C. I. Westbrook, and A. Aspect, Science **292**, 461 (2001).

[48] F. Pereira Dos Santos, J. Léonard, J. Wang, C. J. Barrelet, F. Perales, E. Rasel, C. S. Unnikrishnan, M. Leduc, and C. Cohen-Tannoudji, Phys. Rev. Lett. **86**, 3459 (2001).

[49] P. F. Bedaque, E. Braaten, and H.-W. Hammer, Phys. Rev. Lett. **85**, 908 (2000).

[50] S. L. Cornish, N. R. Claussen, J. L. Roberts, E. A. Cornell, and C. E. Wieman, Phys. Rev. Lett. **85**, 1795 (2000).

[51] K. E. Strecker, G. B. Partridge, A. G. Truscott, and R. G. Hulet, Nature (London) **417**, 150 (2002).

[52] T. Weber, J. Herbig, M. Mark, H.-C. Nägerl, and R. Grimm, Science **299**, 232 (2003).

[53] M. Landini, S. Roy, G. Roati, A. Simoni, M. Inguscio, G. Modugno, and M. Fattori, Phys. Rev. A **86**, 033421 (2012).

[54] J. L. Roberts, N. R. Claussen, S. L. Cornish, and C. E. Wieman, Phys. Rev. Lett. **85**, 728 (2000).

[55] A. L. Marchant, S. Händel, S. A. Hopkins, T. P. Wiles, and S. L. Cornish, Phys. Rev. A **85**, 053647 (2012).

[56] V. Efimov, Phys. Lett. B **33**, 563 (1970).

[57] E. Braaten and H.-W. Hammer, Phys. Rep. **428**, 259 (2006).

[58] T. Kraemer, M. Mark, P. Waldburger, J. G. Danzl, C. Chin, B. Engeser, A. D. Lange, K. Pilch, A. Jaakkola, H. C. Nägerl, and R. Grimm, Nature (London) **440**, 315 (2006).

[59] M. Berninger, A. Zenesini, B. Huang, W. Harm, H.-C. Nägerl, F. Ferlaino, R. Grimm, P. S. Julienne, and J. M. Hutson, Phys. Rev. Lett. **107**, 120401 (2011).

[60] C. J. Myatt, E. A. Burt, R. W. Ghrist, E. A. Cornell, and C. E. Wieman, Phys. Rev. Lett. **78**, 586 (1997).
[61] G. Modugno, M. Modugno, F. Riboli, G. Roati, and M. Inguscio, Phys. Rev. Lett. **89**, 190404 (2002).
[62] Z. Hadzibabic, C. A. Stan, K. Dieckmann, S. Gupta, M. W. Zwierlein, A. Görlitz, and W. Ketterle, Phys. Rev. Lett. **88**, 160401 (2002).
[63] G. Roati, F. Riboli, G. Modugno, and M. Inguscio, Phys. Rev. Lett. **89**, 150403 (2002).
[64] C. Silber, S. Günther, C. Marzok, B. Deh, P. W. Courteille, and C. Zimmermann, Phys. Rev. Lett. **95**, 170408 (2005).
[65] S. B. Papp, J. M. Pino, and C. E. Wieman, Phys. Rev. Lett. **101**, 040402 (2008).
[66] H.-W. Cho, D. J. McCarron, M. P. Köppinger, D. L. Jenkin, K. L. Butler, P. S. Julienne, C. L. Blackley, C. R. Le Sueur, J. M. Hutson, and S. L. Cornish, Phys. Rev. A **87**, 010703 (2013).
[67] F. Riboli and M. Modugno, Phys. Rev. A **65**, 063614 (2002).
[68] B. Damski, L. Santos, E. Tiemann, M. Lewenstein, S. Kotochigova, P. Julienne, and P. Zoller, Phys. Rev. Lett. **90**, 110401 (2003).
[69] C.-L. Hung, X. Zhang, N. Gemelke, and C. Chin, Phys. Rev. A **78**, 011604 (2008).
[70] D. J. McCarron, H. W. Cho, D. L. Jenkin, M. P. Köppinger, and S. L. Cornish, Phys. Rev. A **84**, 011603 (2011).
[71] G. Roati, M. Zaccanti, C. D'Errico, J. Catani, M. Modugno, A. Simoni, M. Inguscio, and G. Modugno, Phys. Rev. Lett. **99**, 010403 (2007).
[72] E. A. Burt, R. W. Ghrist, C. J. Myatt, M. J. Holland, E. A. Cornell, and C. E. Wieman, Phys. Rev. Lett. **79**, 337 (1997).
[73] C. Chin, T. Kraemer, M. Mark, J. Herbig, P. Waldburger, H.-C. Nägerl, and R. Grimm, Phys. Rev. Lett. **94**, 123201 (2005).
[74] J. Herbig, T. Kraemer, M. Mark, T. Weber, C. Chin, H.-C. Nägerl, and R. Grimm, Science **301**, 1510 (2003).
[75] M. Mark, T. Kraemer, J. Herbig, C. Chin, H.-C. Nägerl, and R. Grimm, Europhys. Lett. **69**, 706 (2005).
[76] B. DeMarco and D. S. Jin, Science **285**, 1703 (1999).